Check for updates

The effect of microwave hydrothermal treatment on the combustion behavior of sewage sludge

Zechen Jin[1], Qian Zhang[1,2,3], Fengxiang Qiu[1], Weijie Hu[1], Yuheng Feng[2,3]* and Shuping Zhang[4]*

[1]Shanghai Municipal Engineering Design Institute (Group) Co., Ltd., Shanghai, China, [2]Thermal and Environmental Engineering Institute, School of Mechanical Engineering, Tongji University, Shanghai, China, [3]Shanghai Engineering Research Center of Multi-Source Solid Wastes Co-Processing and Energy Utilization, Shanghai, China, [4]School of Energy and Power Engineering, Nanjing University of Science and Technology, Nanjing, Jiangsu, China

In this study, the thermal behavior of microwave hydrothermal char of sewage sludge (MTC) was compared with dried sludge (DS) and char produced by electric hydrothermal treatment (ETC). The retention ratio of volatile matter in MTC was raised by 51.2% compared with in HTS, while their dewaterability by centrifugation were very close. The kinetic parameters of thermal disposal process of the DS and hydrochars were determined from TG analysis. It was found that the activation energy of combustion was reduced from 44.20 kJ/mol of DS to 47.29 kJ/mol for ETC. For MTC, the activation energy was slightly decreased (43.22 kJ/mol). In addition, the highest weight loss rate (0.49%/min) in combustion was also found for MTC. The evolution of gaseous nitrogen compounds was obtained by FTIR analyzer combined with TG. The results indicated that in devolatilization process, the emission of NH_3, the main precursor of NOx in combustion, was postulated to higher temperature for MTC. In conclusion, MTC has a better combustion performance and a close dewaterability compared with to ETC. This study provided a new choice for the pre-treatment method of sewage sludge before combustion.

KEYWORDS

sewage sludge, microwave, kinetic analysis, hydrothermal treatment, pyrolysis, combustion

Introduction

With the rapid urbanization in China, a large amount of sludge (SS) is generated from sewage treatment every year. The dried sludge production has reached 11.6 million tons in 2020 (China, 2020). Landfilling and composting take up a large amount of land resources and produces leachate containing heavy metals that may pollute groundwater. As for anaerobic digestion, its treatment cycle is long and the digestate is difficult to use in agriculture. Sludge as a biomass with high carbon content, is gaining attention as an

energy resource (Zuo, 2023). Incineration completely breaks down organic matter in SS in short period thus attracts more attention these days.

The raw SS from water treatment plants has a large water content. Therefore, a moisture removal process is necessary before incineration. Hydrothermal treatment is a cost-effective method because it largely reduces the energy consumption of the mechanical drying process. It also improves the fuel quality of SS as fuel and reduces NO emissions (Zhao et al., 2013). In recent years, the use of microwaves as an energy source for hydrothermal treatment has attracted the attention of scholars because it can effectively heat uniformly. Moreover, this pre-treatment has a lower risk of heavy metal loss (Wang et al., 2022a). However, no previous study systematically compared the microwave and traditional hydrothermal treatments on the combustion performance of SS.

In this study, SS was treated using hydrothermal reactor by microwave and electric heating respectively. The incineration and pyrolysis characterization of the raw sludge, dried sludge and treated sludges was analyzed by TG-FTIR analysis. The effect of microwave hydrothermal pre-treatment on the sludge incineration performance was discussed. The results of this study provide basic data for the optimization of pretreatment methods for SS incineration.

Materials and methods

Materials

Raw SS with a moisture content of 80.4%, was sampled from a water treatment plant in Shanghai, China. The samples dried for 24 h in an oven at 105°C were crushed and packed in sample bags to ensure the dryness, labeled with DS.

Hydrothermal reaction

The raw sludge microwave hydrothermal treatment was performed in microwave digestion reactor (MDS-6G, Sineo, Shanghai). And the raw sludge was treated in a subcritical hydrothermal reactor with electric heater as the control group. Since hydrothermal reactions at 200°C result in higher organic retention (Jin et al., 2020), more energy-rich hydrothermal carbon (Kim et al., 2015), and less tar production during pyrolysis (Feng et al., 2018a), final temperature was set at 200°C with the heating rate 10°C/min for both the treatments. The residence time for the final temperature was 0.5 h. The slurry left in the reactor was centrifuged at 6000 revolutions/min for 10 min. The wet char separated was dried at 105°C for 12 h. The char from electric and microwave hydrothermal treatment are

labelled with ETC and MTC, respectively. The thermal behavior of semi-dried sludge (SDS) was used to compared with the DS to understand the effect of thermal drying process usually at around 100°C before sludge incineration. The SDS was prepared by drying raw sludge for 12 h.

Analytical methods

The thermal behavior of the sludge and hydrochar during incineration and pyrolysis was characterized by TG-FTIR analysis which was carried out using a TA Instruments Q500 and a NICOLET iS10 with air and nitrogen as carrier gas respectively, at a flow rate of 100 ml/min. The wavenumber range of FTIR analyzer is 600–4000 and ackground scan time is 8 Scans.

Results and discussion

Chemical composition of hydrochars

The proximate and elemental analysis based on dry base of DS, ETC and MTC are listed in Table 1. It could be found that the yield of MTC was higher than ETC. The recovery of VM in MTC was 58.2% higher than that in ETC, mainly due to the less volatile release to liquid and gas phase for MTC. The enhanced charring of the organic compounds in liquid by microwave heating is another possible reason. Close moisture contents were found for the two hydrochars, indicating that microwave and electric hydrothermal treatment had similar effects on the promotion of dewaterablity of SS.

From Van Krevelen diagram in Figure 1, it could be found that dehydration was dominant volatile loss reaction for MTC while for ETC it is a mixture of decarboxylation and dehydration. Compared with MTC, the location of ETC in the diagram is significantly further to DS due to high extent of decarboxylation, which was corresponding to both the high volatile and oxygen reduction of MTC. The loss of hydrophilic groups such as carboxylation and hydroxyl groups contributed to the dewaterability of hydrochar (Feng et al., 2018a). The close dewaterability of the two hydrochars despite the long distance in Van Krevelen diagram indicated that dehydration played a dominant role in moisture removal of the chars here.

Themogravimetric analysis of SS samples

Figure 2 showed the TG and DTG curves of DS and chars for pyrolysis/combustion processes at the heating rate of 10°C/min. It could be found that the pyrolysis process of the SS samples before and after pretreatment can be briefly divided into four stages according to the DTG curves, i.e., stage 1 from

TABLE 1 The proximate and elemental analysis of DS, ETC and MTC.

	Ash (wt%)	Volatile (wt%)	Fixed carbon (wt%)	Moisture content (wt%)	Yield (%/DS)	Volatile fraction retention (%/DS)
DS	53.60	40.99	5.41	80.00	100.00	100.00
ETC	64.59	28.83	6.58	65.84	72.95	51.31
MTC	59.54	37.01	3.45	66.10	89.89	81.15
	N (wt%)	C (wt%)	H (wt%)	S (wt%)	O (wt%)	
DS	2.75	19.65	3.39	0.54	20.08	
ETC	2.19	17.31	2.45	0.50	12.96	
MTC	2.47	17.52	2.75	0.58	17.14	

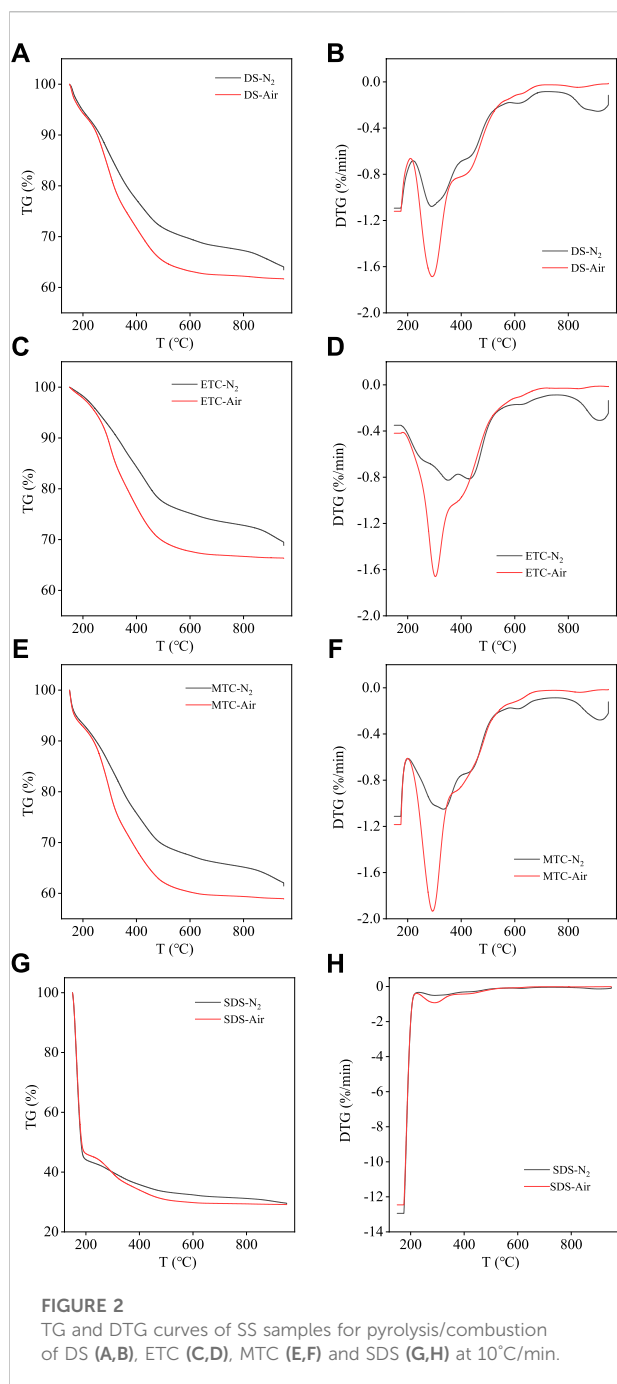

FIGURE 1
Van Krevelen diagram of SS samples.
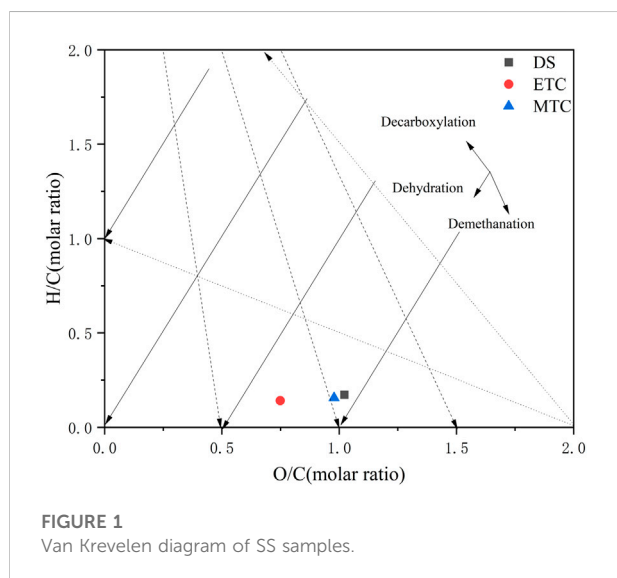
ambient temperature to 200°C was the moisture loss stage, mainly the removal of internal water (Qian et al., 2011); stage 2 from 200 to 500°C was the main volatilization stage of the organic matter contained in the SS, including the decomposition of proteins, sugars and fatty compounds (Naqvi et al., 2019); stage 3 from 500 to 700°C was the decomposition of a small amount of stabile organic components, such as the expulsion of polycyclic aromatic hydrocarbons (PAHs) (Hu et al., 2020); stage 4 with the temperature above 800°C was mainly caused by the decomposition of inorganic substances. Comparing different samples, it can be found that hydrothermal pretreatments have significant impact on the pyrolysis process. Table 2 showed the indexes of pyrolysis and combustion performance of different SS samples. Hydrothermal and microwave hydrothermal pretreatment can increase the peak temperature (T_p) from 292.17°C for dry SS to 354.50°C for ETC and 335.33°C for MTC, respectively. Meanwhile, the average weight loss rate was also increased from 0.43%/min for DS to 0.47%/min for ETC and to 0.48%/min for MTC Furthermore, hydrothermal pretreatment of SS effectively improved the volatile release index (D) for pyrolysis process. These results indicated that hydrothermal or microwave hydrothermal pretreatment changed the organic matters, averaged the composition, and thus improved the reaction characteristics for pyrolysis process of SS.

As shown in Figure 2, the combustion process of SS samples can be briefly divided into three stages according to the TG and DTG process, including moisture loss stage, main volatilization stage; and char combustion stage (Lin et al., 2015). Compared with the pyrolysis process, the combustion process did not show the decomposition process of inorganic substances. This could be attributed to the promotion of mineral decomposition in the presence of oxygen, which shifted the corresponding weight loss peak to lower temperature so it could not be identified separately in DTG curve. From Table 2, it was found that electric hydrothermal pretreatment decreased the values of D from $6.26 \times 10^{-8}\%^2 \text{ min}^{-2} \cdot °C^{-3}$ for dry SS to $4.33 \times 10^{-8}\%^2 \text{ min}^{-2} \cdot °C^{-3}$ for ETC, which was attributed to the fact that hydrothermal process dissolved part of the active organic components so reduced the combustion reactivity (Wilk et al., 2019). However, microwave hydrothermal pretreatment retained 81.15% of the organic matter in MTC sample, increasing the D value to $8.32 \times 10^{-8}\%^2 \text{ min}^{-2} \cdot °C^{-3}$. This was probably due to the reduction of the stability of volatile matters in SS by microwave treatment.

Kinetic analysis of SS samples

Kinetic parameters of pyrolysis and combustion of different SS samples based on Coats-Redfern method were presented in Table 3, 4 respectively. High correlation coefficients ($R^2 > 0.97$) for all the processes indicated that the first order reaction model [$F(\alpha) = -\ln(1-\alpha)$] was well suited to the weight loss curves of pyrolysis and combustion of different samples. By comparing the parameters of DS and SDS, it was found that the water contained

FIGURE 2
TG and DTG curves of SS samples for pyrolysis/combustion of DS **(A,B)**, ETC **(C,D)**, MTC **(E,F)** and SDS **(G,H)** at 10°C/min.

in SS had little effect on the pyrolysis process. Whereas, electric hydrothermal pretreatment significantly increased the pyrolysis activation energy, to 57.14 kJ/mol. During electric hydrothermal pretreatment process, some labile organic components released from the sample, while some catalytic alkali metal elements leached into liquid phase, leading to the higher activation energy of ETC (Tasca et al., 2019). For MTC, the activation energy was slightly increased to 51.61 kJ/mol, which was due to the recovery of labile organic matter as mentioned in TG

analysis. Similarly, water contained in SS has little effect on the combustion process due to the nearly identical activation energies of DS and SDS (E = 44.20 kJ/kg for DS and E = 44.44 kJ/kg for SDS). It was also found that hydrothermal pretreatment increased the combustion activation energy from 44.20 kJ/kg for SS to 47.29 kJ/kg for ETC. However, the activation energy decreased to 43.22 kJ/kg for MTC, indicating that microwave hydrothermal pretreatment promoted the combustion process and lowered its reaction barrier. The possible reason was that the retention of labile organic compounds in hydrochar and the leaching of inorganic components that hinder combustion (Udayanga et al., 2019; Wang et al., 2022b). Microwave hydrothermal pretreatment retained recovered 81.15% of the organic matter in MTC sample, increasing its combustion reaction index. In general, microwave hydrothermal pretreatment was more favorable for improving the combustion performance of SS.

Release characteristics of N-containing gaseous compounds

Figure 3 presented the NH_3 release curves according to the absorbance of N-H bending vibration at 966 cm^{-1} during SS pyrolysis and combustion process from the FTIR spectra. In the case of DS, it was found from Figure 3A that NH_3 started to release from around 150°C and reached the peak release amount at 284°C with the main release stage of 150–500°C during pyrolysis process. The peak at 270°C and 555°C was due to the decomposition of labile protein and stable protein respectively. For ETC and MTC, the release of NH_3 was delayed to around 250°C, and the main release phase was extended to 700°C. Both of the two peaks shifted to higher temperature. This was attributed to that the stabilized the protein structure leading to its suspended decomposition (JunZhang and Zuo, 2013). The other reason was the release of inorganic-N and part of labile protein-N into liquid phase during the treatment (Feng et al., 2018b). In addition, the hydroxyl radicals derived from SS hydrothermal pretreatment process can damage the extracellular polymers, which protected proteins from high temperature depolymerization (He et al., 2015; Feng et al., 2018b). For the combustion process in Figure 3B, different shape of NH_3 emission curves was found compared with pyrolysis process below 650°C. Above 650°C, minor release occurred due to the oxidation. The close peak temperature at around 460°C was found in the combustion of different SS samples. The net emission of NH_3 was reduced by 65.8% and 62.3% for ETC and MTC compared with DS, respectively. Therefore, both electric and microwave hydrothermal treatment significantly inhibited the release of NH_3 during combustion process of SS.

TABLE 2 Indexes of pyrolysis and combustion performance of different SS samples.

Samples	WL^a	T_i^b	T_p^c	$\Delta T_{1/2}^d$	$-DTG_{mean}^e$	$-DTG_{max}^f$	D^g (Chen et al., 2022)
	%	°C	°C	°C	%/min	%/min	$\%^2 \, min^{-2} \cdot °C^{-3}$
DS-N_2	35.56	225.67	292.17	177.67	0.43	1.09	1.44×10^{-8}
DS-Air	38.36	215.00	298.33	186.33	0.44	1.69	6.26×10^{-8}
ETC-N_2	31.21	179.83	354.50	197.83	0.47	0.83	2.41×10^{-8}
ETC-Air	33.71	197.33	305.67	251.50	0.48	1.66	4.33×10^{-8}
MTC-N_2	38.58	198.67	335.33	486.67	0.48	1.11	1.48×10^{-8}
MTC-Air	41.12	205.83	288.67	178.50	0.49	1.93	8.32×10^{-8}

[a]WL: Weight loss ratio.
[b]T_i: Initial decomposition temperature.
[c]T_p: Peak temperature (the temperature corresponding to the maximum weight loss rate).
[d]$\Delta T_{1/2}$: Half-peak width temperature (-DTG/-DTGmax = 0.5).
[e]-DTG_{mean}: Average weight loss rate.
[f]-DTG_{max}: Maximum weight loss rate.
[g]-volatile release index, D = ($DTG_{mean} \cdot DTG_{max}$)/($T_i \cdot T_p \cdot \Delta T_{1/2}$)

TABLE 3 Pyrolysis kinetic parameters of different SS samples based on Coats-Redfern method.

Samples	F(α)	Fitting formula	R^2	E (kJ/mol)
SS-N_2	-ln(1-α)	y = -6.06x-4.10	0.978	49.33
	$(1-α)^{-1}-1$	y = -10.30x-2.90	0.976	83.84
	$[(1-α)^{-2}-1]/2$	y = -15.70x-11.77	0.936	127.80
	$α^2$	y = -7.95x-2.43	0.885	61.78
	α+(1-α)ln(1-α)	y = -9.36x-0.73	0.926	76.19
	α	y = -3.31x-8.72	0.836	26.94
ETC-N_2	-ln(1-α)	y = -7.02x-2.90	0.984	57.14
	$(1-α)^{-1}-1$	y = -10.97x-3.56	0.971	89.30
	$[(1-α)^{-2}-1]/2$	y = -15.93x-11.66	0.928	129.67
	$α^2$	y = -10.04x-0.37	0.918	81.73
	α+(1-α)ln(1-α)	y = -11.45x-2.04	0.948	93.20
	α	y = -4.35x-7.32	0.891	35.41
MTC-N_2	-ln(1-α)	y = -6.34x-3.73	0.974	51.61
	$(1-α)^{-1}-1$	y = -10.60x-3.30	0.972	86.28
	$[(1-α)^{-2}-1]/2$	y = -16.02x-12.19	0.935	130.40
	$α^2$	y = -8.45x-1.74	0.881	68.78
	α+(1-α)ln(1-α)	y = -9.88x-0.01	0.922	80.42
	α	y = -3.56x-8.36	0.835	28.98
SDS-N_2	-ln(1-α)	y = -5.98x-4.18	0.976	48.68
	$(1-α)^{-1}-1$	y = -10.31x-2.97	0.973	83.92
	$[(1-α)^{-2}-1]/2$	y = -15.83x-12.05	0.938	128.86
	$α^2$	y = -7.73x-2.72	0.874	62.92
	α+(1-α)ln(1-α)	y = -9.15x-1.00	0.918	74.48
	α	y = -3.20x-8.86	0.82	26.05

TABLE 4 Combustion kinetic parameters of different SS samples based on Coats-Redfern method.

Samples	F(α)	Fitting formula	R^2	E (kJ/mol)
SS-Air	-ln(1-α)	y = -5.43x-4.97	0.988	44.20
	$(1-α)^{-1}-1$	y = -9.66x-2.03	0.963	78.63
	$[(1-α)^{-2}-1]/2$	y = -15.07x-10.94	0.921	122.67
	$α^2$	y = -6.78x-4.06	0.917	55.19
	α+(1-α)ln(1-α)	y = -8.16x-2.40	0.952	66.42
	α	y = -2.73x-9.53	0.871	22.22
ETC-Air	-ln(1-α)	y = -5.81x-4.39	0.991	47.29
	$(1-α)^{-1}-1$	y = -10.40x-3.20	0.970	84.66
	$[(1-α)^{-2}-1]/2$	y = -16.29x-12.88	0.930	132.60
	$α^2$	y = -7.17x-3.48	0.909	58.36
	α+(1-α)ln(1-α)	y = -8.62x-1.71	0.947	70.17
	α	y = -2.92x-9.25	0.863	23.77
MTC-Air	-ln(1-α)	y = -5.31x-5.12	0.991	43.22
	$(1-α)^{-1}-1$	y = -9.60x-2.00	0.966	78.14
	$[(1-α)^{-2}-1]/2$	y = -15.10x-11.08	0.927	122.91
	$α^2$	y = -6.49x-4.44	0.917	52.83
	α+(1-α)ln(1-α)	y = -7.87x-2.78	0.953	64.02
	α	y = -2.58x-9.73	0.868	20.35
SDS-Air	-ln(1-α)	y = -5.46x-4.90	0.991	44.44
	$(1-α)^{-1}-1$	y = -9.84x-2.35	0.965	80.10
	$[(1-α)^{-2}-1]/2$	y = -15.44x-11.58	0.924	125.68
	$α^2$	y = -6.71x-4.14	0.916	54.62
	α+(1-α)ln(1-α)	y = -8.11x-2.45	0.953	66.02
	α	y = -2.69x-9.58	0.869	21.90

Only the spectra of DS combustion shows the characteristic bands of HCN around 714 and 3342 cm^{-1}, which were corresponding to the C-H bending and N≡CH stretching respectively. Figure 4A displayed the spectrum of gaseous product from DS combustion at 400°C (Wang et al., 2009; Yang et al., 2015; Li et al., 2017). This meant that hydrothermal treatment
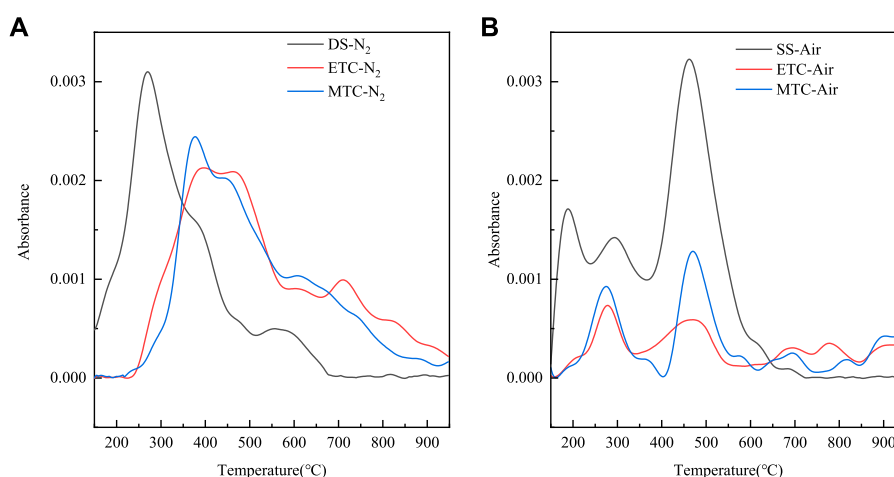
FIGURE 3
NH3 release curves during **(A)** pyrolysis and **(B)** combustion process of different SS samples.
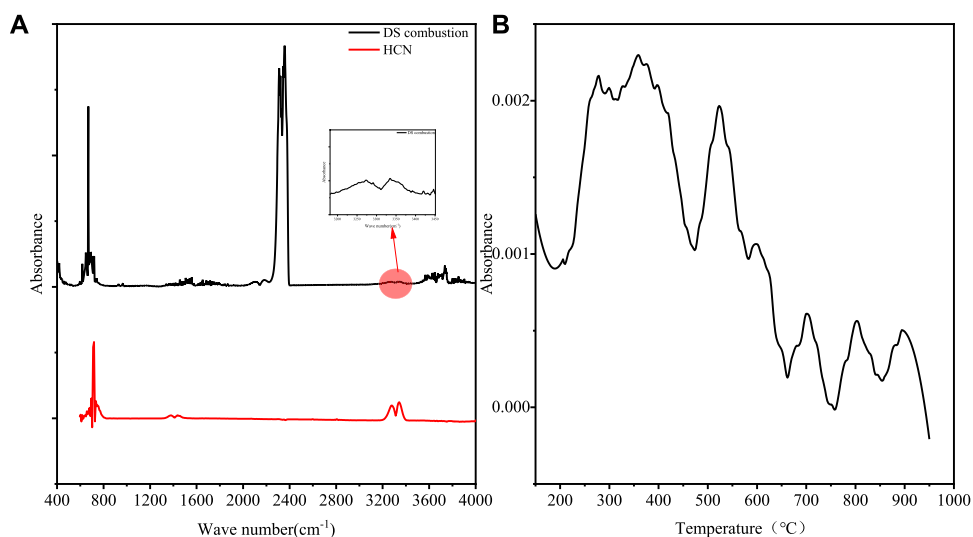
FIGURE 4
(A) The spectrum of gaseous products from DS combustion 400°C and HCN; **(B)** the release curves of DS combustion at 3342 cm^{-1} wave number absorption with temperature.

inhibited the formation of nitrile and heterocyclic-N compounds, which were the precursors of HCN in the following combustion process (Feng et al., 2020; Xu et al., 2023). On the other side, compared with pyrolysis, the presence of oxygen in atmosphere promoted the formation of HCN at low temperature. Since the band around 714 cm^{-1} is overlapped with the band of CO_2, the absorbance of the second highest peak at 3342 cm^{-1} was used to analyze the evolution of with temperature as in Figure 4B. There were generally two steps for HCN emission. The first was from

189 to 473°C while the second was from 473 to 663°C. At higher temperature, few HCN emission was found since its oxidation (Jiang et al., 2010).

Conclusion

The TG analysis of SS samples pretreated by different methods showed that the activation energy of combustion was increased

from 44.20 kJ/mol for DS to 47.29 kJ/mol for ETC, while decreased to 43.22 kJ/mol for MTC. In addition, the highest average weight loss rate (0.49%/min) in combustion was also found for MTC. The high recovery of active organic compounds in MTC was the main reason. The FTIR results indicated that in devolatilization process, the emission of NH_3 was postulated to higher temperature for MTC, mainly due to the stabilization of protein compounds during hydrothermal treatment. In conclusion, MTC has a better combustion performance and a close dewaterability compared with to ETC (Zuo et al., 2023).

Data availability statement

The raw data supporting the conclusions of this article will be made available by the authors, without undue reservation.

Author contributions

ZJ, QZ, and FQ contributed to the conception and design of the study. ZJ organized the experiments. QZ performed the statistical analysis. YF wrote the first draft of the manuscript.

WH and SZ wrote parts of the manuscript. All authors participated in the revision of the manuscript, read and approved the submitted version.

Conflict of interest

Authors ZJ, QZ, FQ, and, WH were employed by Shanghai Municipal Engineering Design Institute (Group) Co., Ltd.

The remaining authors declare that the research was conducted in the absence of any commercial or financial relationships that could be construed as a potential conflict of interest.

Publisher's note

All claims expressed in this article are solely those of the authors and do not necessarily represent those of their affiliated organizations, or those of the publisher, the editors and the reviewers. Any product that may be evaluated in this article, or claim that may be made by its manufacturer, is not guaranteed or endorsed by the publisher.

References

China, N. B. O. S. (2020). *China Urban-Rural construction statistical yearbook*, Springer, Berlin/Heidelberg, Germany,

Chen, M., Zhang, S., Su, Y., Niu, X., Zhu, S., and Liu, X. (2022). Catalytic co-pyrolysis of food waste digestate and corn husk with CaO catalyst for upgrading bio-oil. *Renew. Energ.* 186, 105–114.

Feng, J. A., Xz, A., Hui, L. B., Jl, A., Gxbc, D., and Hao, L. A. (2020). Effect of regeneration conditions on the emission of HCN in FCC regeneration process. *Chem. Eng. J.* 389, 124484. doi:10.1016/j.cej.2020.124484

Feng, Y., Yu, T., Chen, D., Xu, G., Wan, L., Zhang, Q., et al. (2018). Effect of hydrothermal treatment on the steam gasification behavior of sewage sludge: Reactivity and nitrogen emission. *Energ Fuel*, 32, 1, 581–587. doi:10.1021/acs.energyfuels.7b03304

Feng, Y., Yu, T., Ma, K., Xu, G., Hu, Y., Chen, D., et al. (2018). Effect of hydrothermal temperature on the steam gasification performance of sewage sludge: Syngas quality and tar formation. *Energ Fuel*, 32, 6, 6834–6838. doi:10.1021/acs.energyfuels.8b00696

He, C., Wang, K., Yang, Y., Amaniampong, P. N., and Wang, J. Y. (2015). Effective nitrogen removal and recovery from dewatered sewage sludge using a novel integrated system of accelerated hydrothermal deamination and air stripping. *Environ. Sci. Technol.* 49 (11), 6872–6880. doi:10.1021/acs.est.5b00652

Hu, Y., Xia, Y., Maio, F. D., Yu, F., and Yu, W. (2020). Investigation of polycyclic aromatic hydrocarbons (PAHs) formed in three-phase products from the pyrolysis of various wastewater sewage sludge. *J. Hazard. Mat.* 389, 122045. doi:10.1016/j.jhazmat.2020.122045

Jiang, X., Li, C., Chi, Y., and Yan, J. (2010). TG-FTIR study on urea-formaldehyde resin residue during pyrolysis and combustion. *J. Hazard. Mat.* 173 (1-3), 205–210. https://doi:10.1016/j.jhazmat.2009.08.070

Jin, X., Zhun, F., Qiuying, L., Qi, T., Yang, L., Yaoyao, L., et al. (2020). Characteristics of hydrothermal carbonization products of municipal sludge in mountainous cities. *China Water & Wastewater* 36 (21), 21–27.

Jun Zhang, Wei Zuo, Yu Tian, Tao Tan, Yanni Cui, Lin Chen, (2013). Nitrogen conversion in relation to NH3 and HCN during microwave pyrolysis of sewage sludge. *Environmental Science & Technology Es & T*, 47(7):3498-505. doi:10.1021/es304248j

Kim, D., Lee, K., and Park, K. (2015). Hydrothermal carbonization of sewage sludge for solid recovered fuel and energy recovery. *J. Korean Soc. Water Wastewater* 29 (1), 57–63. doi:10.11001/jksww.2015.29.1.057

Li, X., Chen, L., Dai, X., Mei, Q., and Ding, G. (2017). Thermogravimetry–Fourier transform infrared spectrometry–mass spectrometry technique to evaluate the effect of anaerobic digestion on gaseous products of sewage sludge sequential pyrolysis. *J. Anal. Appl. Pyrolysis* 126, 288–297. doi:10.1016/j.jaap.2017.05.018

Lin, Y., Ma, X., Peng, X., Hu, S., Yu, Z., Fang, S., et al. (2015). Effect of hydrothermal carbonization temperature on combustion behavior of hydrochar fuel from paper sludge. *Appl. Therm. Eng* 91, 574-582.

Naqvi, S. R., Tariq, R., Hameed, Z., Ali, I., Naqvi, M., Chen, W. H., et al. (2019). Pyrolysis of high ash sewage sludge: Kinetics and thermodynamic analysis using Coats-Redfern method. *Renew. Energy* 131 (FEB), 854–860. doi:10.1016/j.renene.2018.07.094

Qian, J., Yoon, Y. W., Youn, P. S., Ji, H. K., Choi, D. S., Choi, J. H., et al. (2011). Drying characteristics of sewage sludge. *Korean J. Chem. Eng.* 28 (7), 1636–1640. doi:10.1007/s11814-011-0009-5

Tasca, A. L., Puccini, M., Gori, R., Corsi, I., Galletti, A., and Vitolo, S. (2019). Hydrothermal carbonization of sewage sludge: A critical analysis of process severity, hydrochar properties and environmental implications. *Waste Manag.* 93 (JUN), 1–13. doi:10.1016/j.wasman.2019.05.027

Udayanga, W., Veksha, A., Giannis, A., Lisak, G., and Lim, T. T. (2019). Effects of sewage sludge organic and inorganic constituents on the properties of pyrolysis products. *Energy Convers. Manag.* 196 (SEP), 1410–1419. doi:10.1016/j.enconman.2019.06.025

Wang, Y., Yu, Y., Huang, H., Yu, C., Fang, H., Zhou, C., et al. (2022). Efficient conversion of sewage sludge into hydrochar by microwave-assisted hydrothermal carbonization. *Sci. Total Environ.* 803, 149874. doi:10.1016/j.scitotenv.2021.149874

Wang, Z., Lv, P., Yuan, H., and Hu, K. (2009). Thermal degradation study of intumescent flame retardants by TG and FTIR: Melamine phosphate and its mixture with pentaerythritol. *J. Anal. Appl. Pyrolysis* 86 (1), 207–214. doi:10.1016/j.jaap.2009.06.007

Wilk, M., Magdziarz, A., Jayaraman, K., Szymanska-Chargot, M., and Gokalp, I. (2019). Hydrothermal carbonization characteristics of sewage sludge and lignocellulosic biomass. A comparative study. *Biomass Bioenergy* 120 (JAN), 166–175. doi:10.1016/j.biombioe.2018.11.016

Xu, K., Li, J., Zeng, K., Zhong, D., Peng, J., Qiu, Y., et al. (2023). The characteristics and evolution of nitrogen in bio-oil from microalgae pyrolysis in molten salt. *Fuel* 331, 125903. doi:10.1016/j.fuel.2022.125903

Yang, J., Chen, H., Zhao, W., and Zhou, J. (2015). TG-FTIR-MS study of pyrolysis products evolving from peat. *J. Anal. Appl. Pyrolysis* 117 (1), 296–309. doi:10.1016/j.jaap.2015.11.002

Zhao, P., Chen, H., Ge, S., and Yoshikawa, K. (2013). Effect of the hydrothermal pretreatment for the reduction of NO emission from sewage sludge combustion. *Appl. Energy* 111(4), 199–205. doi:10.1016/j.apenergy.2013.05.029

Zuo, H., Zeng, K., Zhong, D., Li, J., Qiu, Y., Xu, H., et al. (2023). Multi-dimensional shrinkage models developed by phase field method for gasification of carbonaceous feedstock in packed-bed solar reactor. *Fuel* 331, 125749. doi:10.1016/j.fuel.2022.125749